J. Fluid Mech. (1986), *vol.* 165, *pp.* 221–230
Printed in Great Britain

Gradient destruction in flow through a rigid matrix

By MASSOUD KAVIANY
Department of Mechanical Engineering and Applied Mechanics, University of Michigan, Ann Arbor, Michigan 48109

(Received 5 June 1985)

Fluid flow through a solid matrix is examined by introducing a two-dimensional phenomenological model of flow through a unit cell. The effects of inter-cell mixing on reductions in the upstream prescribed gradients are studied. The velocity gradient is modelled by allowing flows of different average velocities to enter the cell. The exit conditions are then determined by solving for the flow field. It is shown that the extent of the reduction depends on the geometry, Reynolds number and the magnitude of the gradient. Also, some results for reductions in the temperature gradient and a regime diagram for gases are presented.

1. Introduction

In convection through a solid matrix lateral gradients of velocity and temperature can be present, owing to upstream conditions or volumetric sources. A given variation in average velocity between two adjacent pores may become less significant further downstream as the fluid leaving these pores enters a common pore before eventually splitting into separate streams again. The extent of this downstream gradient reduction depends on the structure of the solid matrix, the relative significance of the inertial force, and the magnitude of the gradient, which, in turn, depends on the size of the unit cell in the solid matrix.

The size of the unit cell and the magnitudes of the gradients can determine whether a local volume average of the field equations based on a representative elementary volume can be used. For this to be applicable, the representative elementary volume must contain a sufficient number of pores (saturated with the fluid)† so that the inter-pore mixing mechanism need not be taken into account (Slattery 1972; Carbonell & Whitaker 1984; Hassanizadeh & Gray 1983). This holds true for many saturated porous media where the pore size is very small. For these media the Reynolds number based on the lengthscale of the unit cell is relatively low. Also, even if the gradients throughout the system are large, the variations in velocity and temperature across a unit cell are rather insignificant. As a result, for very small unit-cell dimensions, large gradients can be sustained in the medium.

In treatments similar to the one described here, the flow through solid matrices has been studied for predictions of the permeability (Barak & Bear 1981), deviations from Darcy's model at high Reynolds numbers due to detaching of the flow (Barak & Bear 1981; Stark 1972) and dispersion of tracers (Hinduja, Sundaresan & Jackson 1980; Carbonell & Whitaker 1983).

In this paper, based on a two-dimensional phenomenological model, the

† This study is limited to flow of a single-component and single-phase fluid through a solid matrix with periodic microstructure.

mechanisms of inter-pore mixing and the related significant parameters are studied. The model is based on laminar flow through an isotropic and non-consolidated rigid matrix. The entrance to the unit cell consists of two ports through which the fluid flows at different velocities. These flows mix† in the cell and then exit through similar ports at the opposite side of the cell. The Navier–Stokes equation describing this flow system is solved numerically through finite-difference approximations. The flow is assumed to remain attached in passing through the cell; therefore, the results are limited to lower Reynolds numbers.

2. A phenomenological model

Figure 1 (*a*) shows the mode to be considered here. The two streams, u_1 and u_2, both Poiseuille flows at $x = 0$, enter the cell, travel over the back step, impinge on the forward steps forming stagnation flows and then move toward the centre of the cell and mix. For mathematical simplicity, symmetry is assumed at $y = 0$ and $y = 2+c/a$, and fully developed flows are assumed at the entrance ($x = 0$) and exit ($x = (d_i+d_f)/a+2b/a+e/a$). The symbols are defined in figure 1. Depending on the value of b/a the flows can accelerate or decelerate when passing through this section. Next, they move through the central channel, become partially developed and then enter the second chamber, where they impinge on the forward step forming a stagnation flow, split and leave through the two exits.

When non-dimensionalized by applying a (this choice will be explained later), $(\bar{u}_1+\bar{u}_2)$, and $\rho(\bar{u}_1+\bar{u}_2)^2$ to scale length, velocity and pressure, the continuity and momentum equations for laminar, constant properties and steady-state flows are

$$u_x+v_y = 0, \tag{1}$$

$$uu_x+vu_y = -p_x+2Re^{-1}(u_{xx}+u_{yy}), \tag{2}$$

$$uv_x+vv_y = -p_y+2Re^{-1}(v_{xx}+v_{yy}), \tag{3}$$

where subscripts x and y indicate differentiation, p is pressure, u and v are the longitudinal and lateral velocity components respectively, $Re = 2\bar{u}a/\nu$ is the Reynolds number, $\bar{u} = \bar{u}_1+\bar{u}_2$, the overbar indicating spatial average, and ν is the kinematic viscosity.

The boundary conditions for this model are:

entrance: $$u_{1,i} = f(y), \quad u_{2,i} = g(y), \quad p = p_i, \tag{4}$$

symmetry planes: $$v = u_y = p_y = 0, \tag{5}$$

exit: $$u_{x,f} = 0, \quad p_{xx,f} = 0, \tag{6}$$

solid boundaries: $$u = v = 0, \tag{7}$$

where i indicates entrance and f indicates final conditions. The average velocities are

$$\bar{u}_1 = \int_0^1 u(y)\,dy, \quad \bar{u}_2 = \int_{1+c/a}^{2+c/a} u(y)\,dy, \tag{8}$$

so that $$\bar{u}_1+\bar{u}_2 = 1.$$

The entrance profiles $f(y)$ and $g(y)$ are prescribed Poiseuille velocity profiles. The magnitude of $\bar{u}_{1,i}$ is specified; then $\bar{u}_{2,i} = 1-\bar{u}_{1,i}$ and $\Delta\bar{u}_i = (\bar{u}_{1,i}-\bar{u}_{2,i})$. At the exit

† The flow 'mixing' is not meant as a vortex or turbulent mixing.

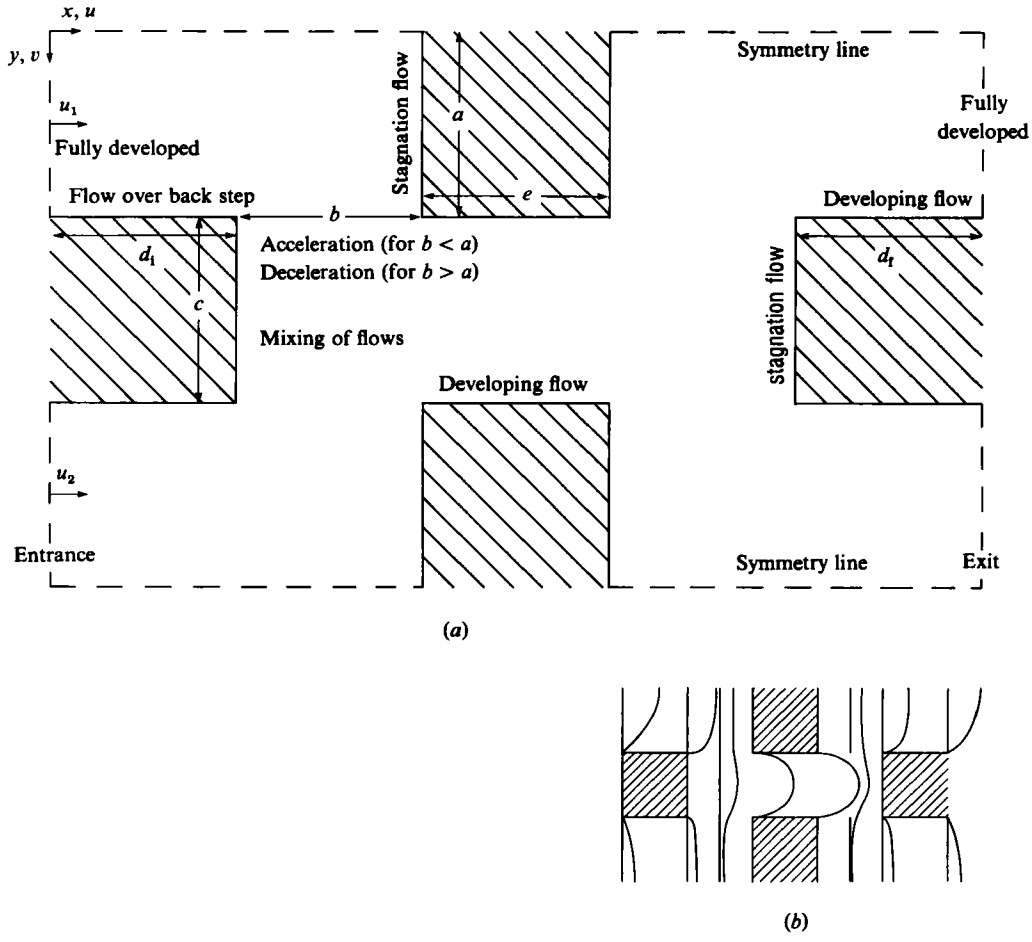

FIGURE 1. (*a*) Schematic of the unit cell considered and (*b*) an example of the distribution of the longitudinal velocity at various locations; $\Delta\bar{u}_1 = 0.5$, $Re = 0.5$.

the average velocities are computed using the trapezoidal rule (even though the flow is nearly Poiseuille in all cases).

The integration of (1)–(3) subject to (4)–(7) is done numerically through finite-difference approximations using a combination of a pressure-correction technique, the power-law approximation and the staggered-grid system, as recommended in Patankar (1980). This method has been successfully used for the study of flow through porous inserts (Kaviany 1985). A uniform grid net of $\Delta y = \Delta x = 0.1$ was used. The standard convergence validation, using progressively finer grid nets, was applied and the results showed complete convergence. However, the grid net used here proved to be relatively accurate and computationally economical. A review of the literature on flow over steps (Stark 1972; Durst, Melling & Whitelaw 1975; Sinha, Gupta & Oberai 1981; Rockwell & Naudascher 1979; Dalman, Merkin & McGreavy 1984) indicates that the flow remains attached and steady for the range of Reynolds numbers considered in this study.

3. Results and discussion

Even though the distance between the two streams c is taken to be finite in the model, it is expected that the results should also hold for very small values of c such that the reduction in Δu can be viewed as a reduction in the gradient.

The results of the numerical integration are given below. Figure 1(b) shows an example of the longitudinal velocity distribution at various locations for $\Delta\bar{u}_i = 0.5$, $a = b = c = d_i = d_f = e$ and $Re = 0.5$.

Figure 2 shows the change in Δu between the entrance and exit for various Reynolds numbers. The results, which are for $a = b = c = d_i = d_f = e$, show that the difference between $\Delta\bar{u}_i$ and $\Delta\bar{u}_f$ increases as $\Delta\bar{u}_i$ or Re increase. For a given $\Delta\bar{u}_i$ and for $0 < Re < 0.5$ the values of $\Delta\bar{u}_f/\Delta\bar{u}_i$ do not change significantly with Re. For $Re > 0.5$ the inertial force becomes progressively more significant as Re increases. As will be shown, the extent of mixing after the first 90° turns depends on the inertial force.

3.1. *Lengthscale*

There are five linear dimensions in the model:

(i) The channel half-width, which is the same as the height of the front step just past the entrance, a. If a is long enough, the flow will be allowed to make a complete turn.

(ii) The length of the entrance section d_i. This length can influence the exit velocities in two ways. First, since the two streams have different velocities but the same pressure at $x = 0$, the pressure drop in each channel depends on d_i and consequently this difference in the pressure drop between the two streams can enhance the mixing. Secondly, the flow over a back step also depends on length d_i. However, as long as it is not significantly smaller than a or b, this upstream condition is not expected to be significant.

(iii) The distance between the back step and forward step b. If b/a is less than unity, the flow accelerates while turning through 90° to enter the common passage. This

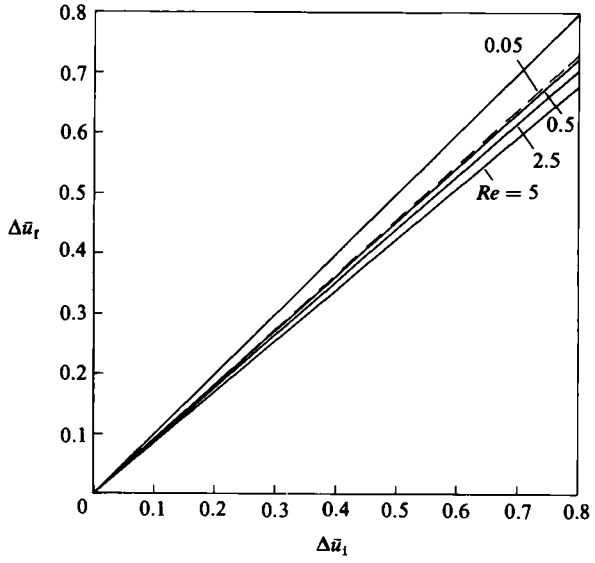

FIGURE 2. The change in the velocity difference for various values of Re and for $a = b = c = d = e$.

results in a further penetration of the flow with larger $\bar{u}$ into the other stream. The reverse takes place for b/a greater than unity.

(iv) The length of the back step at the entrance c. As c/a increases, the two streams travel a longer distance before impingement.

(v) The length of the central channel e. As e/a increases, the combined streams are allowed to develop further. However, the flow through this channel is not the conventional developing flow where at a far enough downstream distance the flow becomes of a boundary-layer type. Instead, the downstream stagnation flow present near the end of the cell influences the flow development in this channel.

(vi) The length of the exit section d_f. This length also has two separate influences on the exit velocities. First, the two streams develop along the length d_f. The dimensionless entrance length (i.e. where the centreline velocity is 99% of its fully developed value) for low-Reynolds-number flow through channels is given as (Chen 1973)

$$\tfrac{1}{2}x_e = \frac{0.63}{0.036Re+1} + 0.044Re, \quad Re = \frac{2\bar{u}a}{\nu}. \tag{9}$$

Therefore, for $0.05 < Re < 5$ considered here, $1.3 < x_e < 1.5$. However, even for $d_f/a = 1$, the flow is nearly fully developed. Secondly, since the two exiting streams have different velocities, the pressure drops they experience along d_f are different, and this would favour an increase in the flow rate of the slower stream. As will be shown this difference in pressure drop along d_f is significant.

Table 1 shows how $\Delta\bar{u}_f/\Delta\bar{u}_i$ varies with changes in $b/a, c/a, d_i/a, e/a$ and d_f/a. While an increase in c/a allows for a greater reduction in the gradient, an increase in b/a results in the opposite. Also given in the table is the tortuosity, defined as the square of the ratio of the path actually taken by the fluid particles L to that taken if the rigid matrix did not exist, L_0 (Dullien 1979). Here it is simply taken to be

$$\left(\frac{L}{L_0}\right)^2 \equiv \left(\frac{2d+2b+e+2a}{2d+2b+e}\right)^2. \tag{10}$$

As can be seen, tortuosity (as used here) does not appear to be the parameter describing the extent of gradient destruction.

Figure 3 shows the influence of the exit length on the difference in exit velocities. The results are for $a = b = c = d_i = e$ and $Re = 0.5$ and 5. Since the pressure drop along d_f is smaller for a slower stream, then the final split of the flow favours the slower stream.

The results presented above show that the significant linear dimensions are a, b and d_f, with a characterizing the channel and primary stagnation flows, b determining the acceleration or deceleration of the flows after the 90° turns, and d_f determining

Geometry	$\left(\frac{L}{L_0}\right)^2$	$\frac{\Delta\bar{u}_f}{(\Delta\bar{u}_f)_{a-b-c-d_i-d_f-e}}$
$a = b = c = d_i = d_f = e$	1.96	1.00
$c = 2a, a = b = d_i = d_f = e$	1.96	0.98
$e = 2a, a = b = c = d_i = d_f$	1.78	1.00
$b = 2a, a = c = d_i = d_f = e$	1.65	1.06
$d_i = 2a, a = b = c = d_f = e$	1.65	1.00
$d_f = 2a, a = b = c = d_i = e$	1.65	0.99

TABLE 1. Exit velocity for several geometric arrangements, $\Delta\bar{u}_i = 0.8$ and $Re = 5$

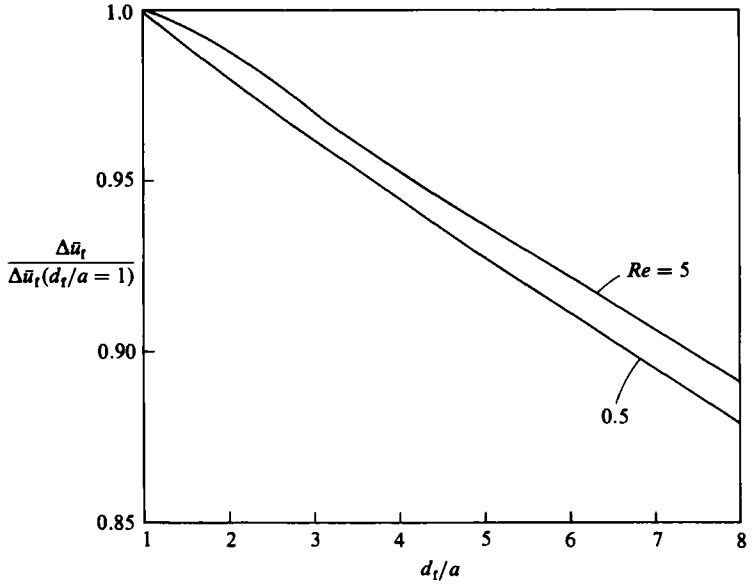

FIGURE 3. Variation of the difference in exit velocities with respect to the length of the exit section d_f. The results are for $a = b = c = d_i = e$, $Re = 0.5$ and 5 and $\Delta\bar{u}_i = 0.8$.

the extent of the difference in pressure drop between the two streams at the exit section.

3.2. *Effect of presence of a wall*

When either of the two symmetry planes is replaced by a rigid boundary, the no-slip conditions cause a relative retardation of the flow near this boundary. There are two possibilities:

Case (i). The faster flow is close to the wall (such as in vertical-plate natural convection if the location of the maximum velocity is in the channel next to the wall).

Case (ii). The slower flow is next to the wall (as in forced convection).

Consider $\Delta\bar{u}_i = 0.8$ and $b = a$. Then the wall can be placed at either $y = 0$ or $y = 3$.† Figure 4 shows $\Delta\bar{u}_f/\Delta\bar{u}_i$ for these two cases, as well as the case with no wall present and for various values of Re. As expected, case (i) results in a more significant gradient reduction, i.e. the presence of the wall causes more reduction if the wall is adjacent to the faster-flowing stream. Therefore, for volumetric sources corresponding to case (i), the gradient reduction is even more significant.

3.3. *Effect of particle size*

For the results to be consistent, they must show that, as the unit-cell size (or the size of the particles making up the matrix) decreases, the gradient reduction becomes insignificant. Available results based on the application of the modified Darcy's law (which includes the inertia and boundary terms) shows that for low permeabilities,‡ i.e. small unit-cell size, relatively large velocity gradients are present adjacent to the

† The entrance velocity profile in the channel adjacent to the wall is Poiseuille with $u(0) = u(1) = 0$, or $u(2) = u(3) = 0$.

‡ In the analysis of flow through porous media, the unit-cell dimension is taken as $(K/\epsilon)^{\frac{1}{2}}$, where K is the permeability (m^2) and ϵ is the porosity. As is shown here, the height of the front step a is the critical cell dimension and it is not yet known how a and other dimensions are related to $(K/\epsilon)^{\frac{1}{2}}$. Some discussion on relating the cell (or particle) size to the permeability is given in Happel & Brenner (1965).

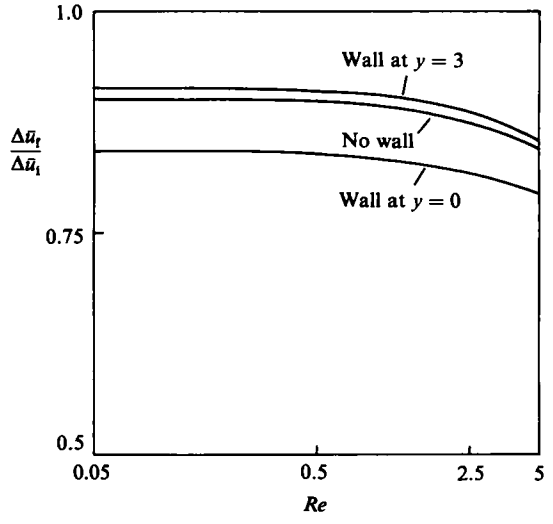

FIGURE 4. The effect of the presence of a wall for $a = b = c = d$, $\Delta\bar{u}_i = 0.8$.

confining impermeable walls (natural convection, Hong, Tien & Kaviany 1985; forced convection, Kaviany 1985).

To demonstrate this, consider two rigid matrices, one with $a = a_I$ and the other with $a = a_{II} = \frac{1}{2}a_I$. Assuming that flows with the same average velocity pass through each of the unit cells, then $Re_{II} = \frac{1}{2}Re_I$. Also, for the same entrance gradient $\Delta\bar{u}_{i,II} = \frac{1}{2}\Delta\bar{u}_{i,I}$. Note that both $\Delta\bar{u}_i$ and Re have decreased for the smaller unit cell, which results in a smaller reduction in the gradient. However, since the smaller cell has half the longitudinal length of the larger cell, the gradient encounters an extra reduction for the same longitudinal length. As an example, for $Re_I = 5$ and $\Delta\bar{u}_{i,I} = 0.8$ the results show $(\Delta\bar{u}_f/\Delta\bar{u}_i)_I = 0.85$ and $(\Delta\bar{u}_f/\Delta\bar{u}_i)_{II} = 0.95$. As $\Delta\bar{u}_i$ decreases, this difference between I and II also decreases.

The above example shows that the solid matrices with a smaller unit-cell size sustain larger lateral gradients.

3.4. *Heat transfer*

If the two entering streams each has a different specific enthalpy, the exit thermal-energy flow rates can be compared with those at the entrance. A non-dimensional average energy flow rate is defined as

$$\bar{T}_1 \equiv \int_0^1 Tu\,dy, \tag{11}$$

where T is the temperature.

A similar expression is used for $\bar{T}_2$. For simplicity, we assume that (a) thermal conductivity of the solid and fluid are equal, and (b) axial conduction is negligible. Then we have

$$uT_x + vT_y = 2Re^{-1}Pr^{-1}T_{yy}, \tag{12}$$

where $Pr = \alpha/\nu$ is the Prandtl number and α is the thermal diffusivity.

This is subject to:

entrance: $$T_{1,i} = 1, \quad T_{2,i} = 0, \tag{13a}$$

symmetry planes: $$T_y = 0. \tag{13b}$$

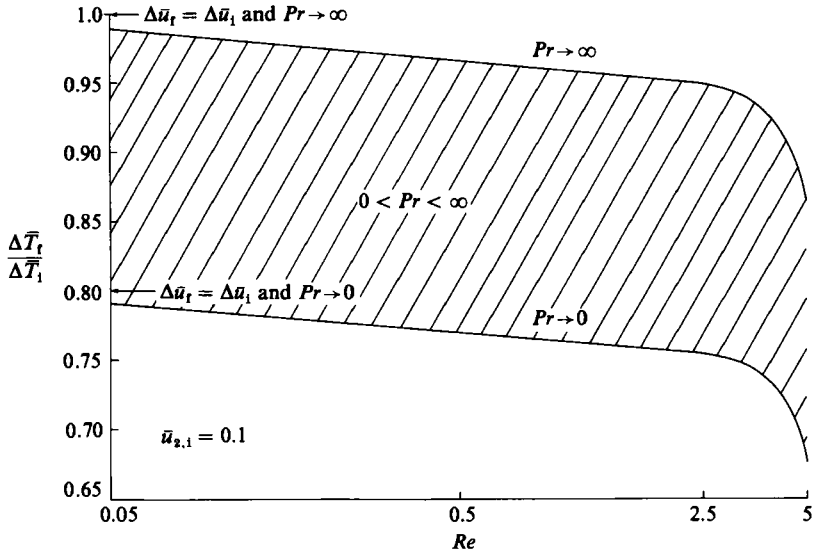

FIGURE 5. Variation in the exit thermal-energy flow rate as $Pr \to 0$ and $Pr \to \infty$ and for $a = b = c = d = e$.

Note that, owing to this lateral symmetry and to the absence of axial conduction, the net enthalpy transport is by convection only. However, the magnitude of the Prandtl number (or the Péclet number = $Re\,Pr$) determines the extent of lateral temperature non-uniformity.

Two cases of special interest are for $Pr \to 0$ and $Pr \to \infty$.

(i) As $Pr \to 0$ the lateral diffusion dominates the convection and the temperature field becomes uniform. This is the upper limit for the interaction between the two streams. For this case we have

$$\frac{\Delta\bar{T}_f}{\Delta\bar{T}_i} = \frac{(\bar{u}_{1,f} - \bar{u}_{2,f})\,T_f}{\bar{u}_{1,i}} \tag{14}$$

where

$$T_f = \frac{\bar{u}_{1,i}}{\bar{u}_{2,f} + \bar{u}_{1,f}} = \bar{u}_{1,i}.$$

(ii) As $Pr \to \infty$ the transfer of energy from one stream to the other is only by convection. This is the lower limit for the interaction between the two streams. For this case we have

$$\frac{\Delta\bar{T}_f}{\Delta\bar{T}_i} = \frac{\bar{u}_{1,f} - (\bar{u}_{2,f} - \bar{u}_{2,i})}{\bar{u}_{1,i}}. \tag{15}$$

The results for these cases and for $b = a$ and $\Delta\bar{u}_i = 0.8$ are given in figure 5. For $Re > 3$, i.e. as the inertial force becomes significant, the thermal-energy exchange between the two streams increases. This behaviour has previously been observed by others in the study of interstitial heat transfer in porous media (Dybbs & Edwards 1984).

3.5. *Regime diagram for gases*

It is of interest to approximately define the regime over which the gradient reduction is significant. This depends on (i) cell structure and dimensions, (ii) the magnitude of velocity, (iii) the magnitude of the gradient, and (iv) the fluid. The results obtained

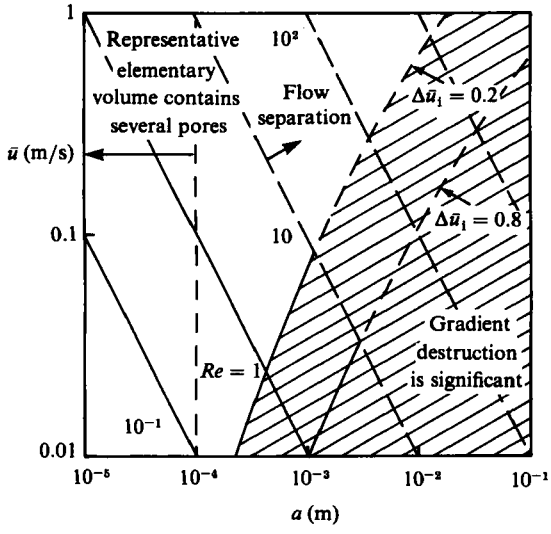

FIGURE 6. A diagram showing the regime of significant gradient reduction for gases and for the type of rigid matrix considered here.

here suggest that, rather than adapting the ratio of the pore size to the characteristic dimension of the system in determining the significance of inter-pore mixing, the magnitude of the pore size should be used. For very small particle sizes, the elementary representative volume, used in developing governing differential equations, contains several (i.e. three or more) pores and therefore the reduction in the gradient due to mixing of flows in adjacent pores need not be considered.

Since flows through solid matrices are encountered in many natural and engineering systems, the ranges of cell size, velocity, and velocity gradients are very large. Figure 6 is based on rough approximations of the flow of gases in such systems, and is given as a guiding tool only. At higher values of Reynolds number the flow separation takes place on passing over the steps and non-Darcian behaviours are observed (Stark 1972; Dybbs & Edwards 1984). The results presented here are for relatively small Reynolds number, i.e. $Re \leqslant 5$. Therefore, for higher values of Re the curves are only rough extrapolations (shown by dashed curves). Also, this diagram is based on the particular phenomenological model used, and the structure of the cell has a significant effect on the extent of gradient reduction.

4. Summary

It is shown that, if the linear dimensions of the unit cell in a solid matrix are relatively large, then the inter-cell mixing and the resulting reduction in the gradients may be significant. Based on the model studied, it was determined that

(*a*) The most important linear dimensions are:
  (i) the entrance channel width a;
  (ii) the width of the passage after the 90° turns b;
  (iii) the length of the exit channel d_f.

(*b*) The extent of reduction in the lateral gradient depends on:
  (i) the Reynolds number;
  (ii) the magnitude of the gradient.

The reduction becomes more significant as the magnitude of these quantities increases.

(*c*) The solid matrices with smaller linear dimensions can sustain larger lateral gradients.

REFERENCES

BARAK, A. Z. & BEAR, J. 1981 Flow of high Reynolds numbers through anisotropic porous media. *Adv. Water Resources* **4**, 54–66.

CARBONELL, R. G. & WHITAKER, S. 1983 Dispersion in pulsed systems. II. Theoretical developments for passive dispersion in porous media. *Chem. Engng Sci.* **38**, 1795–1802.

CARBONELL, R. G. & WHITAKER, S. 1984 Heat and mass transfer in porous media. In *Fundamentals of Transport Phenomena in Porous Media* (ed. J. Bear & M. Y. Corapcioglu), pp. 123–198. Martinus Nijhoff.

CHEN, R.-Y. 1973 Flow in the entrance region at low Reynolds numbers. *Trans. ASME* I: *J. Fluids Engng* **95**, 153–138.

DALMAN, M. T., MERKIN, J. H. & MCGREAVY, C. 1984 Modeling of the fluid flow and heat transfer at the edge of a fixed bed. *Numer. Heat Transfer* **7**, 429–447.

DULLIEN, F. A. L. 1979 *Porous Media, Fluid Transport and Pore Structure*, Academic.

DURST, F., MELLING, A. & WHITELAW, J. H. 1975 Low Reynolds number flow over a plane symmetric sudden expansion. *J. Fluid Mech.* **64**, 1113–1128.

DYBBS, A. & EDWARDS, R. V. 1984 A new look at porous media fluid mechanics – Darcy to turbulent. In *Fundamentals of Transport Phenomena in Porous Media* (ed. J. Bear & M. Y. Corapcioglu), pp. 199–254. Martinus Nijhoff.

HAPPEL, J. & BRENNER, H. 1965 *Low Reynolds Number Hydrodynamics (with Special Application to Particulate Media)*. Prentice-Hall.

HASSANIZADEH, M. & GRAY, W. G. 1983 General conservation equations for multi-phase systems: 1–3. In *Flow Through Porous Media, Recent Developments* (ed. G. F. Pinder), pp. 1–50. Computation Mechanics Publication.

HINDUJA, M. J., SUNDARESAN, S. & JACKSON, R. 1980 A crossflow model of dispersion in packed bed reactors. *AIChE J.* **26**, 274–281.

HONG, J. T., TIEN, C.-L. & KAVIANY, M. 1985 Non-Darcian effects in vertical-plate natural convection in porous media with high porosities. *Intl J. Heat Mass Transfer* **28**, 2149–2157.

KAVIANY, M. 1985 Laminar flow through a porous channel bounded by isothermal parallel plates. *Intl J. Heat Mass Transfer* **28**, 851–858.

PATANKAR, S. V. 1980 *Numerical Heat Transfer and Fluid Flow*. Hemisphere.

ROCKWELL, D. & NAUDASCHER, E. 1979 Self-sustained oscillations of impinging free shear layers. *Ann. Rev. Fluid Mech.* **11**, 67–94.

SINHA, S. N., GUPTA, A. K. & OBERAI, M. M. 1981 Laminar separating flow over backsteps and cavities, part I: backsteps. *AIAA J.* **19**, 1527–1530.

SLATTERY, J. C. 1972 *Momentum, Energy, and Mass Transfer in Continua*. McGraw-Hill.

STARK, K. P. 1972 A numerical study of the nonlinear laminar regime of flow in an idealized porous medium. In *Fundamentals of Transport Phenomena in Porous Media*, pp. 86–102. Elsevier.